Analytical Thermal Model of Natural-Convection Cooling in Axial Flux Machines

P. Shahriari, R. Perini, *Member*, A. Di Gerlando, *Senior Member*, G.M. Foglia, M. Moallem, *Senior Member*

***Abstract*—An analytical approach is proposed in developing a lumped parameter thermal model for the stator coils of naturally-cooled Axial-Flux Tooth-Coil Permanent-Magnet Machines. The model comprises one tooth, the coil around it, the air channels between coils and the teeth supporting structure; each component is subdivided into cuboidal or arc sub-elements. An expression of the convective exchange coefficient is proposed to take into account the radial position of each tooth. Experimental results validate the proposed model, which can also be used in the design stage of a machine.**

***Index Terms*—Axial Flux Machines, Natural Convection, Inclined Parallel-plate air channels, analytical thermal model, design stage thermal model.**

I. Introduction

Thermal study of electric machines is becoming the subject of a great share of research today due to the designer temptation to design efficient and compact electric machines. In this regard, Permanent Magnet Synchronous Machines (PMSMs) focus the greatest consideration.

Among various types of PMSMs, the thermal study of Axial Flux Machines (AFMs) is quite challenging due to the complex fluid flow regimes resulting from the rotation of the rotor surface facing the stator [1]. AFMs are conventionally studied as a general rotor-stator system by using the developed analytical or empirical correlations for heat convection over the surface of the stator and rotor [1]-[3]. The effect of geometrical parameters including the radius of the surfaces and distance between the surfaces [4]-[5], protrusion of the PMs [6], and the inlet configuration [4] is studied to investigate the fluid flow and heat convection. These studies are based on either Computational Fluid Dynamics (CFD) modeling [7], analytical [8], [9] or empirical [10] approaches. In this regard, [11]-[13] are a joint research where a comprehensive fluid flow study and thermal modeling is presented for AFMs.

Besides the heat convection over the rotor and stator surfaces, joule loss extraction from the stator coils should be investigated. Moreover, although CFD and Finite Element (FE) approaches can be adopted to study heat transfer for a complete geometry of the coils [14], for design purposes these approaches are not viable options due to high computation power and time required. Therefore, a reliable analytical thermal model to study the heat transfer of the machine is better appreciated by the designers.

AFMs are either force-cooled [14], [15] or, in case of natural cooling, specific structures like inlet pipes [16] are employed to increase the flow as a result of rotating shaft and thus increase the heat transfer. In this regard, the thermal modeling of natural-cooled AFMs with no inlet in the structure especially for low-speed applications, like wind generators, has not been addressed in any previous study yet. In this paper, an analytical thermal model is proposed, for the natural convection cooling in AFMs with no air inlet. Such a thermal exchange occurs mainly in the stator, so only the thermal behavior of the stator windings will be analyzed, by choosing a simple operating condition: stand still rotor, and DC supply of the windings.

The adopted model is based on a thermal network and can be used in the design, analysis, and condition monitoring of the AFMs. As known, usually the network approach leads to calculate the average temperatures of the machine portions, in particular of the windings. By means of the developed model, the highest coil temperature can be calculated. This can be regarded also as the hot spot estimation: in fact, the limited extension of the coils, compared with the typical lamination stack extension in a radial flux machine, makes the temperature distribution roughly uniform inside each coil, as will be shown in the paper.

The paper is organized as follows. In Section II, the AFM under investigation is introduced and its dimensions are provided. In Section III, some thermal modeling issues of this type of AFM are reviewed. In Section IV, the concept of general arc/cuboidal element thermal model in modeling the heat conduction in solid parts of the machine is recalled. Section V introduces one possible set of correlations defining the heat convection coefficient for the vertical channels. In Section VI, a methodology to study heat convection for a general inclined parallel-plate channel is proposed. In Section VII, the developed thermal model is applied to predict the temperature of the different coils of the machine, and the calculation results are compared with practical measurements for three different working conditions. Finally, in Section VIII a global heat transfer coefficient for each single tooth is estimated, which takes into account all the thermal paths of the wound tooth, useful in the early design stage of an AFM.

Manuscript received November 11, 2018.

P. Shahriari and M. Moallem are with Department of Electrical and Computer Engineering, Isfahan University of Technology, Isfahan, Iran, Postal Code: 84156-83111. Phone: +98 311 3915381. Fax: +98 311 3912451. Email: moallem@cc.iut.ac.ir; p.shahriarinasab@gmail.com.

R. Perini (corresponding author), A. Di Gerlando, G.M. Foglia are with Energy Department, Politecnico di Milano, via La Masa 34, 20156 Milano, Italy. Email: roberto.perini@polimi.it; antonino.digerlando@polimi.it; gianmaria.foglia@polimi.it. Tel: +39 02 23993714. Fax: +39 02 23998566.

II. Axial Flux Machine Under Investigation

The considered AFPM is a four-stage, 50kW, 70RPM wind generator with concentrated coils (Fig. 1); nevertheless, the analysis is of general validity.

Fig. 2 shows a sketch of the machine, and the main dimensions are summarized in Table I.

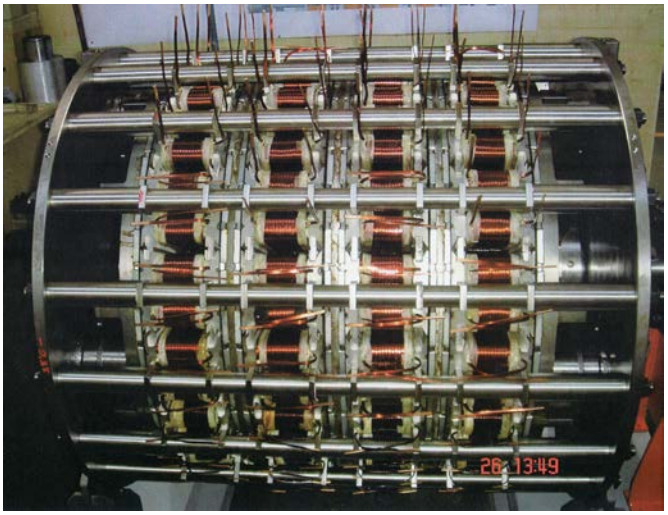

Fig. 1: Detail of the Axial Flux Machine under investigation. It has four-modules and concentrated-coil windings. No air inlet is present.

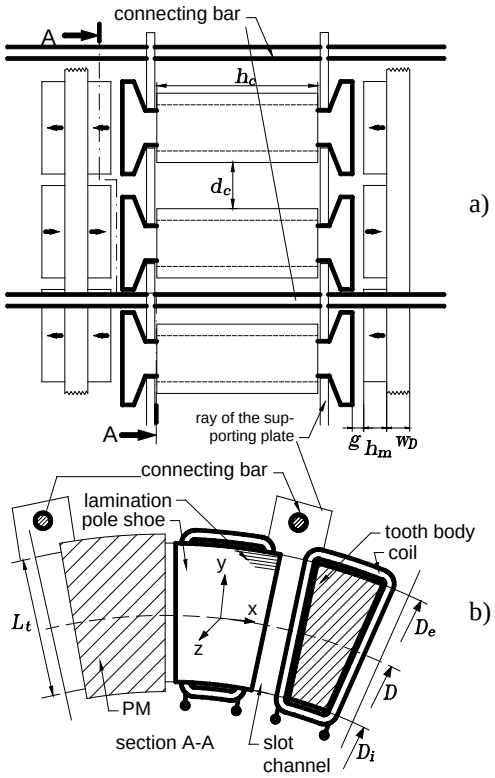

Fig. 2: Structure and main sizes of the machine: a. top view; b. cross section A-A.

Since the rotor is still and the armature currents are DC, the following modelling assumptions have been adopted:

- the effect of rotation on fluid flow is ignored;
- losses in PMs and in iron cores are not taken into account, since fluxes are constant;
- no air inlet is provided.

Further assumption are as follows:

- coils make up parallel-plate air channels;
- heat conduction and natural convection are considered as the means of heat transfer. Radiation is taken into account only for one out of the four surfaces of each coil (the surface which is external in radial direction);
- some model parameters are temperature dependent: thus, the temperature calculation requires an iterative solution.

TABLE I:
RATED VALUES AND MAIN SIZES OF THE MACHINE

Rated P_n [kW], V_n [V], I_n [A], Ω_n [rpm], f_n [Hz]	50, 625, 35, 70, 22.17
No. poles p, No. teeth N_t (one module)	38, 36
D_e, D, D_i, g [mm]	800, 672, 544, 2.5
h_c, L_t, , d_c [mm]	87.5, 128, 10
w_D, h_m [mm]	11, 10

III. Thermal Modelling Issues

The AFM thermal model implies the following issues.

1- For machines with several teeth and then stator air channels, a heat transfer parameter should be introduced for each channel surface. This parameter depends on the surface dimensions, the channel width, the wall temperature of the surfaces and on the channel inclination angle.

2- Since the coils are placed in a radial direction (Fig. 3), on the bottom of the machine the hot air in the channels will be replaced by the ambient air, while on the top of the machine the heated air from the bottom will pass through the channels. This phenomenon should be correctly modelled, as the temperature of the inlet air to the channels affects the channel surfaces temperature.

3- To model heat conduction, an enhanced Lumped Parameter Model (LPM) will be adopted; in fact, usual LPMs are one-dimensional, while the AFM needs a three-dimensional heat conduction model.

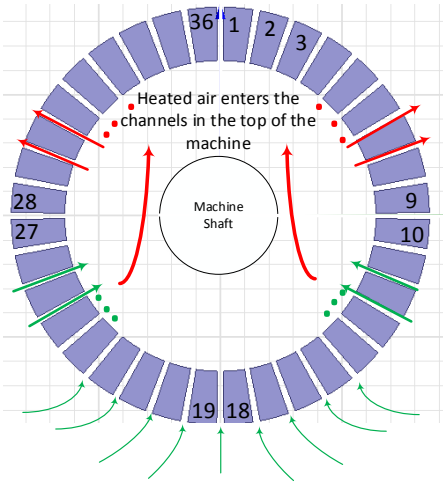

Fig. 3: Graphical representation of the channels and of the fluid flow: green arrows = incoming ambient air; red arrows = outgoing internal air.

IV. Three-Dimensional Heat Conduction Analytical Model Based on General Component Modelling

A. Basic concepts

Heat conduction is governed by the known Fourier's law and heat diffusion equation [20]. However, their solution is not available for all the possible geometries and for most of them it is not possible to find a single solution all over the geometry.

A recently developed study for heat conduction, [18], [19], is based on a three-dimensional analysis applied to a cuboidal or arc element in which the machine can be subdivided.

To develop this analytical model, independent heat flow and uniform heat generation are assumed for each element, which is represented by a single mean temperature. Independent heat flow means that heat cannot change its direction without raising the mean temperature. The solution of the Fourier's law and heat diffusion equation leads to define all the parameters of an equivalent circuit in terms of electrical components.

Fig. 4 shows the model, [18], for a general cuboidal element, where T_{xi}, T_{yi} and T_{zi} (i=1,2) are the temperatures at each end of the element in x, y and z direction respectively, $R_{(x,\,y,\,z)\,i}$ (i=1, 2, 3) are the thermal resistances, $T_{\rm m}$ is the average temperature, C is the thermal capacity, and q is the internal generation of the element. The results are:

$$R_{x1} = R_{x2} = \frac{\ell_x}{2\,k_x\,A_x} \qquad R_{x3} = -\frac{\ell_x}{6\,k_x\,A_x} \tag{1}$$

where ℓ_x, A_x, and k_x are the length, surface section, and thermal conductivity in x-direction, respectively. The same equations can be used for the y- and z-direction by employing respective length, surface, and thermal conductivity.

The model for the arc element is similar to the cuboidal one, but in cylindrical coordinates with peripheral (p), radial (r) and axial (z) directions, Fig. 5. The equations are reported in [19].

All the parts of the machine will be subdivided into either cuboidal- or arc-shaped elements.

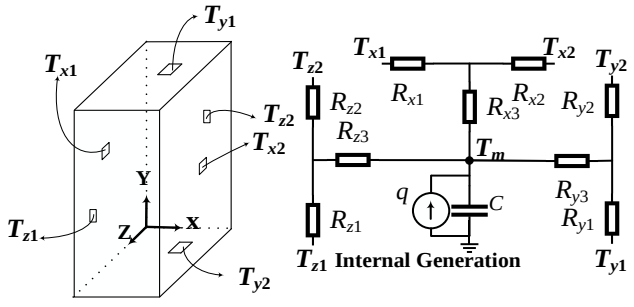

Fig. 4: The graphical representation of a general cuboidal element and its corresponding thermal model.

B. Coil thermal model

The stator of the AFM in this study is electrically and geometrically symmetric as it consists of N_t identical stator tooth-coil combinations. However, it is not thermally symmetric as the heat convection in the channels is not the same for different channels. Here, a simplifying assumption is made by ignoring the interaction of the neighboring teeth. Therefore, only one stator tooth is modeled and the model is solved N_t times by adopting a proper heat convection coefficient for each tooth.

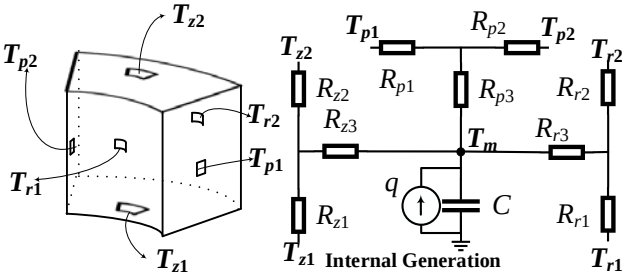

Fig. 5: The graphical representation of a general arc element and its corresponding thermal model.

The coils are not considered as a single isothermal body, but they are divided into four cuboidal elements (Fig. 6a), each one corresponding to one coil side; the model for the top and bottom and for the right and left parts of the coils are shown in Fig. 6b and Fig. 6c respectively. Heat exchange in coils is neglected in the direction with lower surface dimension facing the air (z-direction in Fig. 6).

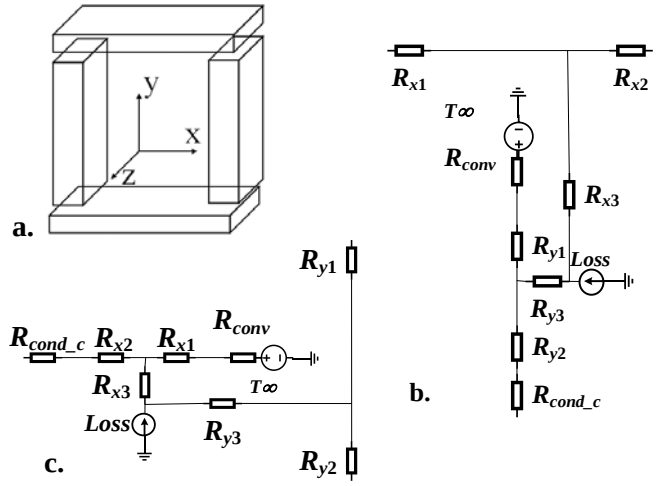

Fig. 6: a thermal model of the coils of AFM; a. the simplified schematic of one coil; b. model for the top and bottom parts of the coil; c. model of the right and left parts of the coil. T∞ is the ambient temperature.

The four parts differ for the losses and the heat convection coefficients towards the air; both these items depend on the coil part temperature, thus they are updated at each iteration.

For each coil part, the Joule loss is calculated based on the coil current and the actual resistivity of the coil part (the four losses are indicated in Fig. 9 by P_{up}, P_{lo}, P_{lf}, P_{rg}).

The heat convection over the surface of the coils to ambient air is modeled as a convective resistance, R_{conv}, which is connected to an ideal voltage source whose amplitude is equal to the temperature of the ambient air. The expression of R_{conv} is the classical one for convective heat exchange. The expression of the convective coefficient to be used in R_{conv} for each part of the coils will be defined in Section V.

The internal surfaces of the coils are connected to the stator teeth by a conduction resistance, R_{cond_c}, which accounts for the conduction in the insulation between the tooth and the coil.

C. Tooth core thermal model

The stator tooth core is modeled as one cuboidal element. In x- and y-direction, this element is connected to the internal surfaces of the coils. The stator is laminated in the y-direction (Fig. 2b), thus an equivalent thermal conductivity k_{eq} of the steel in this direction is evaluated:

$$k_{eq} = \frac{t_{iron}k_{iron} + 2 \cdot t_{ins}k_{ins}}{t_{iron} + 2 \cdot t_{ins}} \qquad (2)$$

where t_{iron} and t_{ins} are the thickness of lamination and insulation, k_{iron} and k_{ins} are the thermal conductivity, 16.27 [W/(m·K)] for steel and 0.5[W/(m·K)] for insulation materials. As regards the z-direction, the tooth head and the rotor are separated by an air gap in which the air is almost still: thus, the main thermal exchange is via the mechanical structure.

D. Mechanical structure thermal model

The stator teeth are held in place by two supporting plates which are fixed together throughout the machine by connecting bars, as shown in fig.7. In particular, each tooth is embraced by two rays of each supporting plate (see fig. 2).

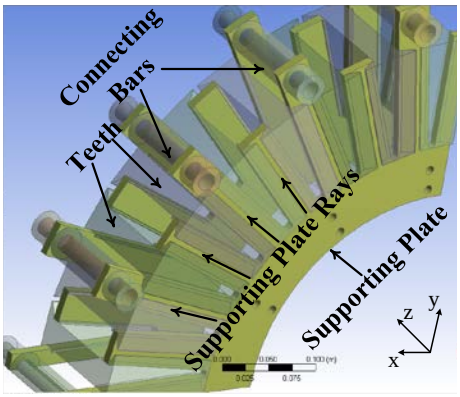

Fig. 7: Supporting plates, rays and connecting bars of the AFM. In this Figure, the coils wound around the teeth are not shown.

Even if the number of connecting bars equals one half of the teeth number, this does not imply any difference in the thermal model of adjacent teeth. Indeed, each tooth has one side in contact with a free ray, and the other side in contact with a ray connected to one connecting bar (fig. 2): adjacent teeth have these rays in reversed positions along the periphery, but the thermal exchange conditions are the same. Thus, also for the heat exchange in the machine structure, a single tooth thermal model approach can be used.

Fig.s 2a and 7 show that both the rays embracing each tooth cannot dissipate heat towards the ambient directly: in fact, the ray surfaces are covered by the tooth heads on one side and by the coil liner on the other side. Thus, the only dissipation path of the rays is the connection with the connecting bars, which can dissipate to the ambient. To model the heat conduction through this path, the z-direction equivalent model of the stator tooth is connected to the bars via a resistance, R_{Plate}, representing the conduction resistance of the ray, and a resistance, R_{cond_p}, which accounts for the conduction in the insulating layer between the tooth and the plate.

Bars are modeled as two-dimensional, axial and radial, arc elements because their structure is annular and heat transfer in the circumferential direction can be disregarded.

The model for the heat exchange in the machine structure is shown in Fig. 8.

E. Wound tooth thermal model

The overall model of one wound tooth is shown in Fig. 9.

In TABLE II, the numerical values of some of the main resistances of the network are reported. The y-direction resistance for the stator tooth is greater than the x- and z-directions due to the lamination.

The model developed for one single coil can be used to study different coils in the AFM by introducing proper heat convection coefficients for different channels. The procedure to define the heat convection inside different inclined channels is presented in Section V.

TABLE II
VALUE OF THE THERMAL RESISTANCES IN THE THERMAL EQUIVALENT CIRCUIT, [K/W]

Left and Right Cuboidal Elements of the coil				
$R_{x1}=R_{x2}$	R_{x3}	$R_{y1}=R_{y2}$	R_{y3}	R_{cont}
$1.6\cdot10^{-2}$	$-5.3\cdot10^{-3}$	$8.1\cdot10^{-2}$	$-2.7\cdot10^{-2}$	$1.3\cdot10^{-1}$
Upper and Lower Cuboidal Elements of the coil				
$R_{x1} = R_{x2}$	R_{x3}	$R_{y1} = R_{y2}$	R_{y3}	R_{cont}
$2.6\cdot10^{-2}$	$-8.6\cdot10^{-3}$	$5.0\cdot10^{-2}$	$-1.6\cdot10^{-2}$	$4.1\cdot10^{-2}$
Connecting Bar Arc Element				
R_{r1}	R_{r2}	R_{r3}	R_{a1}	R_{a2}	R_{a3}	R_{cont-}
$1.6\cdot10^{-3}$	$6.0\cdot10^{-5}$	$-3.0\cdot10^{-4}$	4.2	4.2	-1.4	$3.0\cdot10^{-3}$
Tooth core Cuboidal Element					
$R_{x1} = R_{x2}$	R_{x3}	$R_{y1} = R_{y2}$	R_{y3}	$R_{z1} = R_{z2}$	R_{z3}
$3.0\cdot10^{-2}$	$-1.2\cdot10^{-2}$	11	-3.7	$9.0\cdot10^{-2}$	$-3.0\cdot10^{-2}$

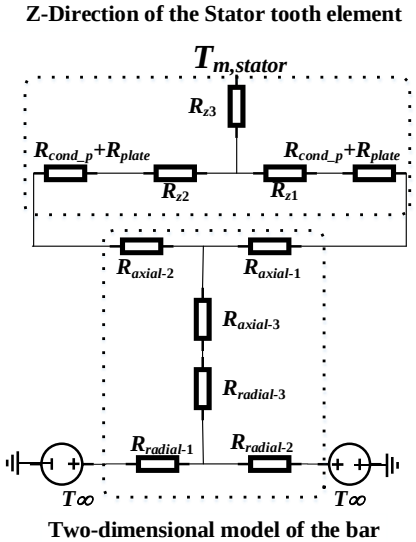

Fig. 8: Thermal model of the machine mechanical structure. T∞ is the ambient temperature.

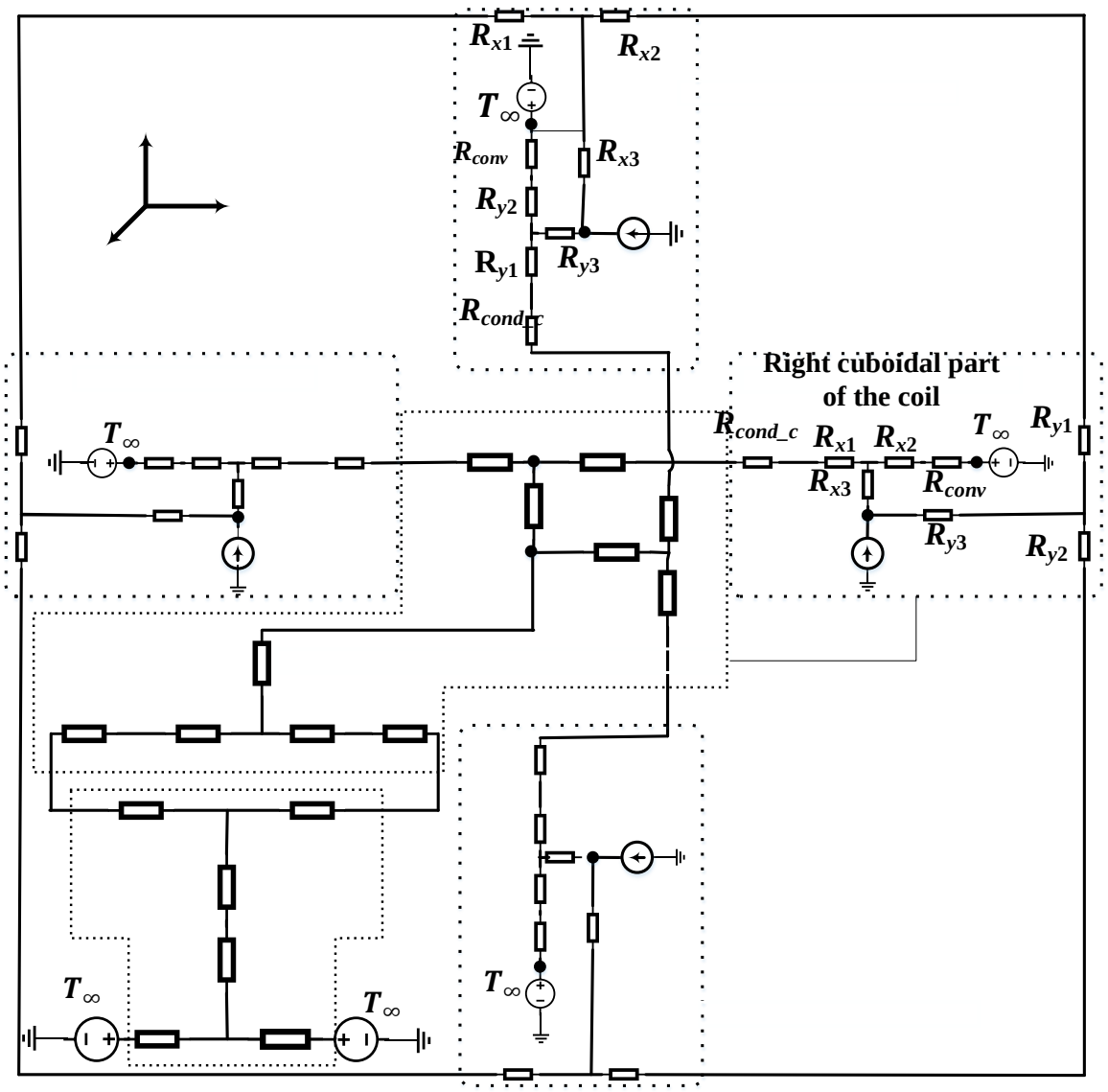

Fig. 9: Proposed equivalent thermal model of the representative thermal part of the machine: a stator tooth, its coil around it (subdivided into four parts), the connecting bars and the supporting plates.

V. Heat Convection in Parallel-Plate Channels

The coil surfaces are hot flat plates interfacing the air which make up temperature boundary layers. The height of the thermal boundary layer is a function of the plate dimension, and of the thermal characteristic of the fluid surrounding the plate. The temperature boundary layers of the plates can mix if the plates are placed close enough to each other, which generates the so-called *"fully developed condition"* regarding the fluid flow inside the channel. In this condition, heat convection for each plate cannot be modeled separately and overall heat convection for the channel should be investigated. On the contrary, when fully developed condition does not occur, the plates do not make up a channel, but they are treated as separated flat plates. Fully developed condition also depends on the inclination of the plates.

In the following, the results of some studies will be reported, concerning both vertical and inclined channels, in fully developed or not fully developed condition.

A. Vertical channels with fully developed condition.

In [20], the correlations for a vertical channel with fully developed condition are reported. The considered channel consists of two plates with length L, supposed isothermal, which are away by the distance $2b$ (

Fig. 10). The fully developed condition is assumed if $Ra \cdot 2b/L \leq 10$, where Ra is the Rayleigh Number. It is a measure of buoyancy-driven flow and is defined as:

$$Ra_l = \frac{g\beta}{\alpha\nu}(T_s - T_\infty)\, l^3 \qquad (3)$$

with Ra_l Rayleigh number for the channel width $l = 2b$, g acceleration of gravity, β =3.66·10^{-3} [K^{-1}] thermal expansion coefficient (equal to inverse of temperature for gases), ν kinematic viscosity (assumed as constant, equal to 17.95·10^{-6} [m^2/s] for air at 25 °C), α thermal diffusivity (assumed as constant, equal to 21.41·10^{-6} [m^2/s] for air at 25 °C), T_s surface temperature, and T_∞ ambient temperature.

Again in [20], a correlation describing the average Nusselt number over the surfaces of vertical parallel-plate channels for isoflux conditions is reported, (4).

$$\overline{Nu} = [\frac{C_1}{(Ra_l\ 2b/L)^2} + \frac{C_2}{(Ra_l\ 2b/L)^{1/2}}]^{-1/2} \quad (4)$$

C_1 =576; C_2 =2.87 (see Fig. 11, crosses).

Finally, the channel convection heat transfer coefficient h can be easily gained, since Nusselt number is the ratio of the convection to the conduction heat transfer coefficients:

$$\overline{Nu} = \frac{h \cdot l}{k_{air}} \quad (5)$$

where, h is the convective coefficient, l is the characteristic length, and k_{air} is the thermal conductivity of the fluid.

B. *Inclined channels.*

Several studies can be cited regarding the analysis of heat convection inside inclined channels, with special geometries and boundary conditions [21]-[26]; here the results of the experimental study [22] are reported.

Fig. 9 in [22], here reported in Fig. 11, shows, for fully developed condition, the channel average Nusselt number as a function of the product between the Rayleigh number Ra and the cosine of the inclination angle θ_{inc}. It is apparent that, for inclination angles 0-80 degrees, the curves converge to a single curve, close to the one for zero inclination (vertical channel). Therefore, the comprehensive correlations that are reported for vertical channels can be adopted by a simple adjustment and replacing the Ra in the correlations with $Ra \cdot \cos(\theta_{inc})$:

$$\overline{Nu_s} = [\frac{C_1}{(Ra_l\ cos(\theta_{inc})\frac{2b}{L})^2} + \frac{C_2}{(Ra_l\ cos(\theta_{inc})\frac{2b}{L})^{\frac{1}{2}}}]^{-1/2} \quad (6)$$

[22] also reports that, when the inclination angle exceeds 80 deg, the Nusselt numbers over the upper and the lower wall differ greatly: this means that in this range it is not possible to obtain one average Nusselt number for the whole channel, i. e. the fully developed condition is not satisfied. The inclined plates making up the channel behave as separated flat plates, and the correlation regarding inclined flat plates must be adopted.

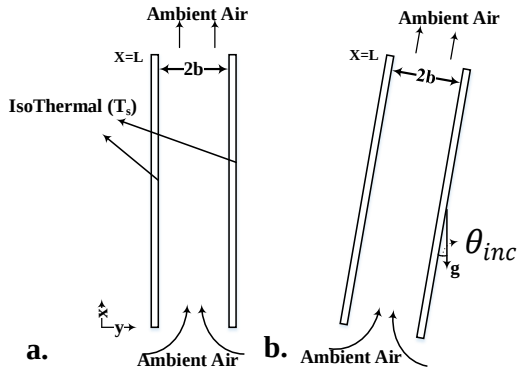

Fig. 10: geometry set up and boundary condition of isothermal parallel-plate air channels: a. vertical channel; b. inclined channel.

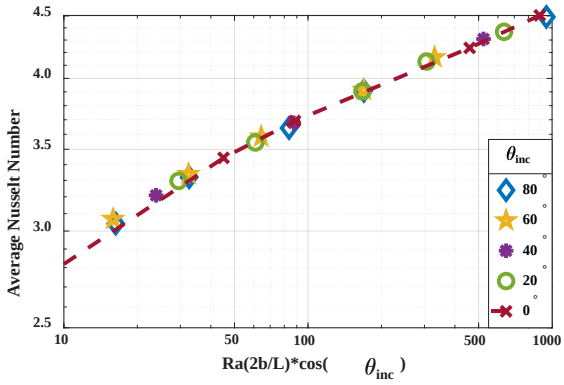

Fig. 11: Average Nusselt number as a function of the product of the Rayleigh number and the cosine of the inclination angle [22] (valid for θ_{inc} = 0-80 deg).

C. *Inclined flat plates.*

A comprehensive set of correlations regarding the inclined flat plates can be found in [27]. In particular, a simple expression for the thermal exchange coefficient is as follows:

$$h_c = 0.68\left(\frac{k_{air}}{L}\right) + 1.31\left[\left(\frac{\Delta T}{k_{air}}\right)cos\vartheta_{inc}\right]^{1/4} \quad (7)$$

where k_{air} is the thermal conductivity of air, ΔT is the temperature difference of the plate and surrounding air, and L is the height of the plate. The formula in (7) is valid for every inclination angle if the flow is laminar.

VI. Proposed Methodology to Model Natural Heat Convection in Inclined Parallel-Plate Channels

By summarizing the results of the previous section:

- [20] gives a geometrical condition for the occurrence of fully developed condition: $Ra{\cdot}2b/L \leq 10$; moreover, it gives correlations for vertical channels in fully developed condition;
- [22] does not give a geometrical condition for the occurrence of fully developed condition, but it shows that, if it occurs, it holds only for a defined inclination interval (0-80 degrees for the geometry in [22]). Moreover, it shows that the correlations valid for vertical channels hold also for inclined channels, by simply replacing Ra by $Ra \cdot \cos(\theta_{inc})$;
- [27] gives some correlations for inclined plates without fully developed condition.

Therefore, the methodology proposed here to study the AFM is as follows:

- assume that fully developed condition occurs if $Ra \cdot \cos(\theta_{inc}) \cdot 2b/L \leq 10$;
- for channels with fully developed condition, adopt the correlations (6) for inclined channels, and evaluate the convection heat transfer coefficient by (5) and (3);
- for channels without a fully developed condition, consider the walls of the channels as separated; since in the AFPM machine the flow is laminar, assume the expression of the convection heat transfer coefficient provided by (7). Note that (7) is used also for coil sides not facing a channel, but faced to free air (upper and lower coil sides in Fig. 9).

As concerns the use of (3) for our channels, the following remarks are valid:

- even if [20] introduced (3) assuming that the channel walls have the same surface temperature T_s, also here we can adopt (3), because the wall temperatures of each channel are not too different between them (a few degrees maximum);
- considering that the model of Fig. 9 is based on a single wound tooth approach, when solving the thermal network of a single coil, the surface temperature T_s is assumed as the one of the coil side faced to the channel.

The adopted assumptions allow to perform the thermal analysis of the machine by solving just one wound tooth at a time instead of solving the whole machine, greatly simplifying the calculations.

The proposed methodology along with the proposed thermal equivalent network is explored for the AFM, and the results are reported in the following section. As mentioned before, the convective parameters are temperature dependent, thus an iterative procedure is necessary.

VII. Model vs Experimental Results

The thermal model in Fig. 9 is considered in this section to estimate the temperature on the coil external surfaces in the AFM.

The solution of the model is an iterative process due to the temperature dependence of the convective coefficients and of the coil losses. To solve the model, the matrix representation of the equivalent network using node analysis is generated.

The iterative calculation algorithm is synthetized in the flow-chart shown in Fig. 12, as will be explained in the following.

The temperature of the input air into the channels must be evaluated carefully.

In the lower machine portion (coils from 11 to 26, whose channels have incoming air, green arrows in Fig. 3) the air entering the channels is the external air: thus, for these channels the input air temperature $T_{air.low}$ equals the ambient temperature T_∞.

On the contrary, the air which reaches the upper coils (coils from 29 to 36 and from 1 to 8, whose channels have outgoing air, red arrows in Fig. 3) is not at temperature T_∞, but at a higher temperature $T_{air.up}$, because ambient air is warmed by the lower coils losses.

Evaluating the amount of the air warming is very challenging: a simplified calculation was tried, to estimate the air speeds in the lower channels and the input-output air flow temperature rises, but unreliable results were found.

In order to obtain an accurate estimation of $T_{air.up}$, a CFD simulation should be performed, but this is outside the scope of the present analysis, for the following reasons:

- a CFD analysis of a so complex system under natural convective conditions is very time consuming, and cannot be regarded as a design tool, especially if a parametric investigation of the machine has to be done;
- a CFD analysis could solve the thermo-fluid field of the overall machine, but it should be considered as an alternative approach with respect to a thermal network method.

Thus, a simplified approach has been adopted, considering that, for sure, the temperature $T_{out.low}$ of the air flow at the output of each lower channel is intermediate between T_∞ and the temperature of the channel walls (corresponding to the coil surfaces temperature T_s).

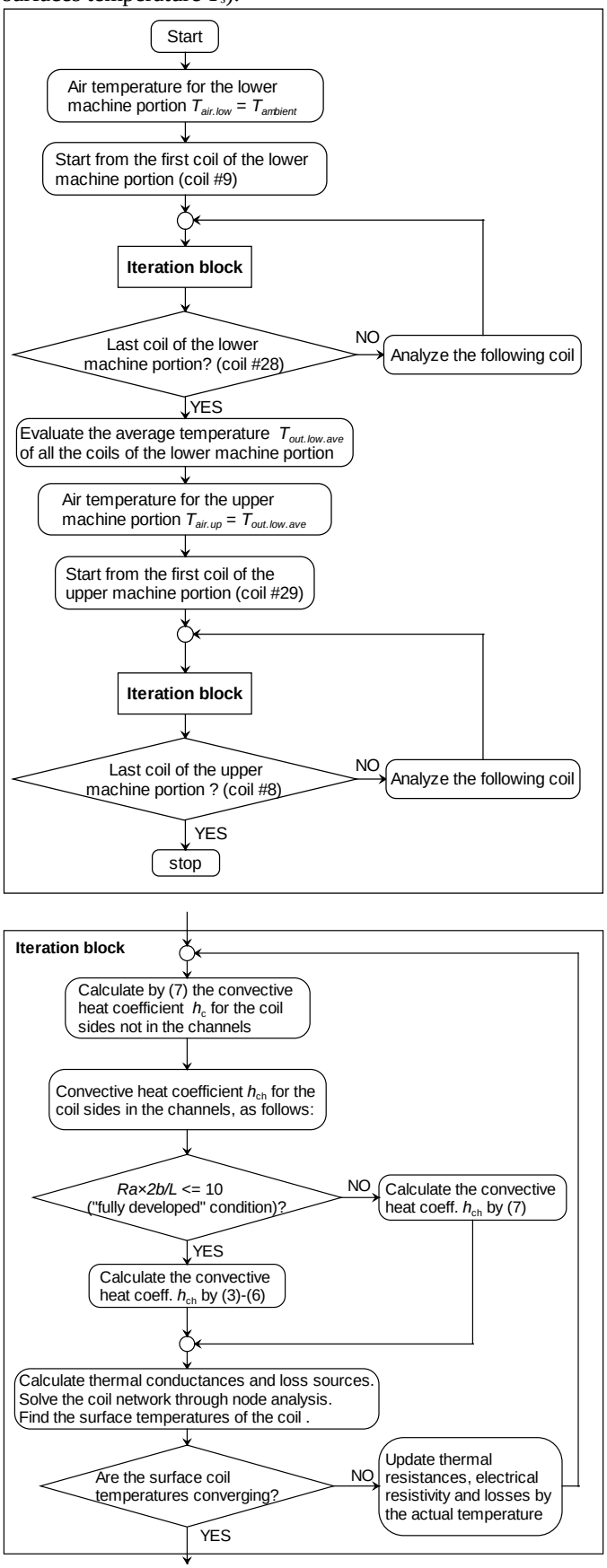

Fig. 12: Flow chart for the iterative calculation of the coil temperatures.

Therefore, for each channel of the lower machine portion, the outgoing air temperature $T_{out.low}$ is estimated as a suited weighted average between T_s and T_∞:

$$T_{out.low} = w \cdot T_\infty + (1 - w) \cdot T_s \quad . \tag{8}$$

Here, the best agreement among calculated and test results were obtained with a weight factor $w = 2/3$.

Finally, the average $T_{out.low.ave}$ among all the $T_{out.low}$ values is assigned to $T_{air.up}$.

As concerns the four coils with horizontal or almost horizontal channels (coils 9, 10, 27, 28), it is assumed that they behave as the lower machine portion coils.

The soundness of the adopted approach is validated by the fair agreement with the measurements on the prototype machine.

Three sets of measurements have been carried out, while the machine coils are excited with dc current by 0.42 p.u., 0.71 p.u., and 1.0 p.u. The ambient temperature is measured for each operating condition and used in the model.

The case when the coils are excited with 0.71 p.u. is initially used to tune the model.

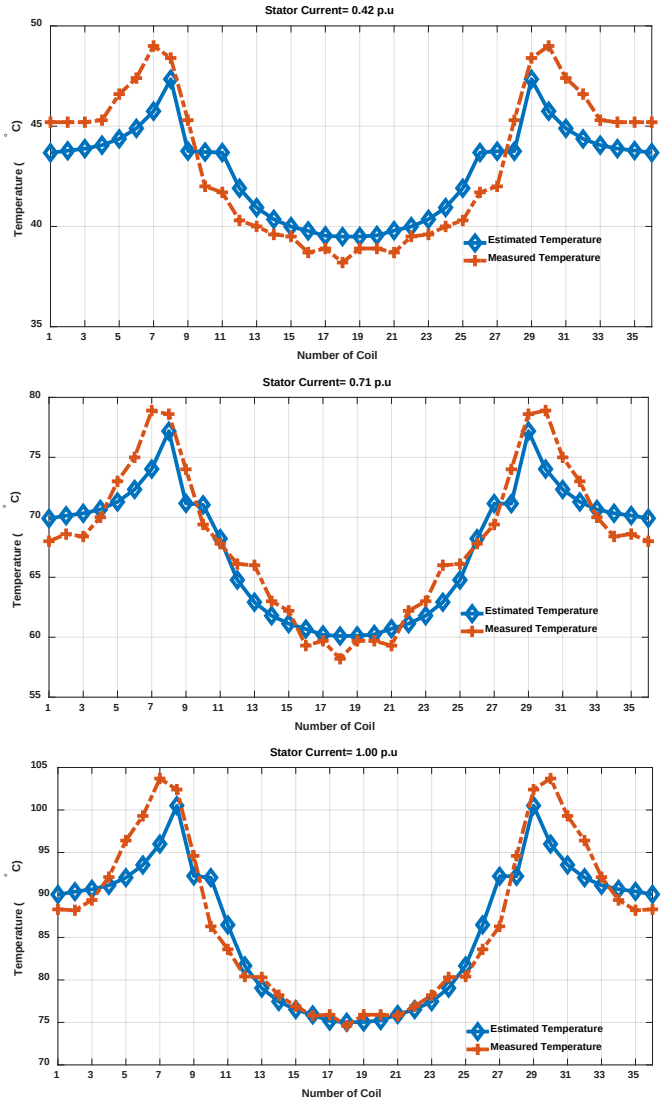

Fig. 13: Estimated and measured temperature of the coils all around the circumference of the machine (refer to Fig. 3).

After this tuning phase, the model is validated with the other two operating conditions (coils excited with 0.42 p.u. and 1 p.u.). For all the three considered operating conditions, Fig. 13 shows the temperature estimation and the experimental values. Even if the thermal model (Fig. 9) considered each coil side as a different body, the model results show that the estimated temperature of the four coil sides ($T_{m,lf}$, $T_{m,rg}$, $T_{m,up}$, $T_{m,lo}$, in Fig. 9) is in practice the same: for the worst case (machine in rated conditions), the average temperature among the four sides differs by less than 0.4 % with respect to each side temperature. This is due both to the very high copper conductivity and to the limited coil size; thus, hereafter the coil is assumed as isothermal, and its temperature is indicated by T_c ; therefore, for each coil, the hot-spot temperature is very close to the average one.

The experimental coil temperature is measured by a thermal laser temperature gun on the coil side which is external in radial direction.

The model overestimates the temperatures of the horizontal coils (No. 9, 28), but is able to predict the temperature of all the other coils with a good precision: the error reaches 18% for the horizontal coils, but it ranges from -4% to +6% for the inclined.

VIII. Global Heat Coefficient Estimation

The thermal model developed in the previous Sections allows to predict both the surface temperature and the loss in each coil. If the loss is divided by the coil external surface and by the coil temperature rise (calculated with respect to the local air temperature, $T_{air.low}$ and $T_{air.up}$ for lower and upper coils respectively), a global convection coefficient h_{wt} can be evaluated for each wound tooth, which takes into account the global thermal exchange of the wound tooth. It is a simplified approach, which can be very useful in early design stage.

Such a global convection coefficient h_{wt} behaves as the channel convection coefficient, that is it depends both on the channel inclination θ_{inc}, and on the coil temperature T_c .

By analyzing the dependence of h_{wt} on θ_{inc} and T_c, it appears that both the dependences can be assumed as quadratic. Thus, the coefficient h_{wt} can be expressed as:

$$h_{wt}(\theta_{inc}, T_c) = k_1\theta_{inc}^2 + k_2\theta_{inc} + k_3T_c^2 + k_4T_c + k_5 \tag{9}$$

where θ_{inc} is expressed in mechanical degrees, T_c in [°C] and h_{wt} in [W/(m^2·K)].

The parameters of (9) are obtained by fitting the thermal model results; two different parameter sets are obtained for the upper and the lower coils respectively, reported in Tab. III.

TABLE IIIII:
Best fitting parameters of (9), identified with 25 °C ambient temperature.

Eq. (9) parameters	k_1	k_2	k_3	k_4	k_5
Upper coils	–0.0011	0.032	–0.0015	0.316	4.270
Lower coils	–0.0006	0.015	–0.0018	0.328	0.309

These parameters hold when the ambient temperature is about 25°C, that is the typical ambient temperature for air cooling in mild climate.

Fig. 14 shows the global wound tooth heat coefficients h_{wt} as a function of the channel inclination angle, for the tested load conditions, both obtained from the complete thermal model of Fig. 9 and from (9). The following remarks are valid:

– a fair agreement between the two kinds of curves exists;
– when increasing the load conditions, the global heat coefficient increases, as typical of natural cooling;
– for the same inclination angle and load conditions, the global heat coefficient of the upper wound teeth is higher with respect to that of the lower one.

The behavior described in the last remark can be explained by observing that the power dissipated in the channels of the upper wound teeth is proportional to the temperature rise with respect to $T_{air.up}$, while the power dissipated by the associated structure portions (connecting bars and supporting plate rays in Fig. 7) is delivered to the air at ambient temperature $T_{air.low}$, thus giving a higher contribution to the global heat coefficient.

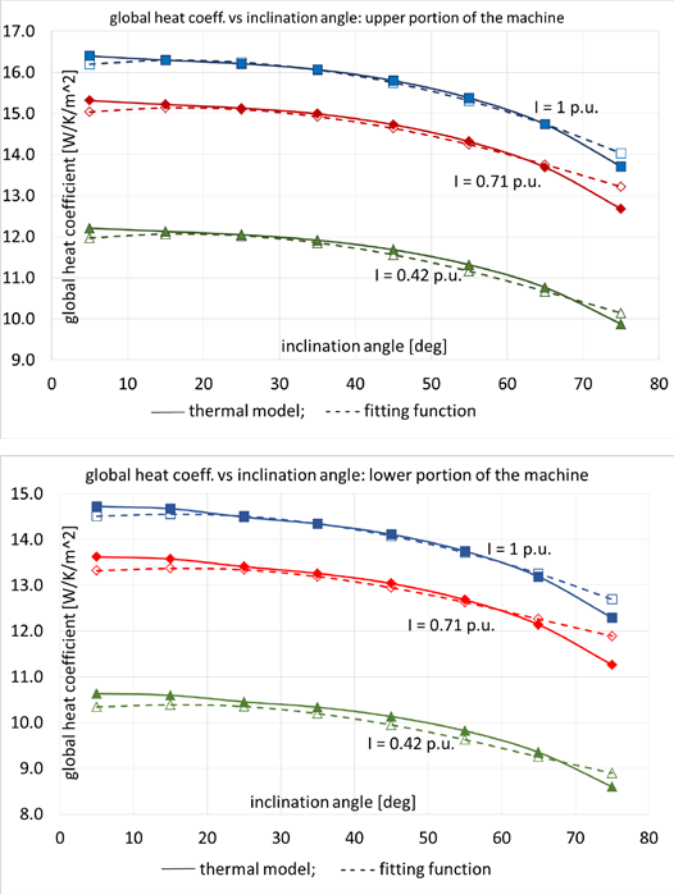

Fig. 14 – Global wound tooth heat convection coefficient for upper and lower portion of the machine, for three working conditions. It holds for θ_{inc}=0-80 deg. (—— = Fig. 9 thermal model; - - - = fitting function (9))

Fig. 15 shows the comparison between the measurements (the same of Fig. 13) and the results of the proposed fitting functions.

The agreement is sufficiently good to allow a rough estimate of the thermal state of the coils in the early design stage of an AFPM machine.

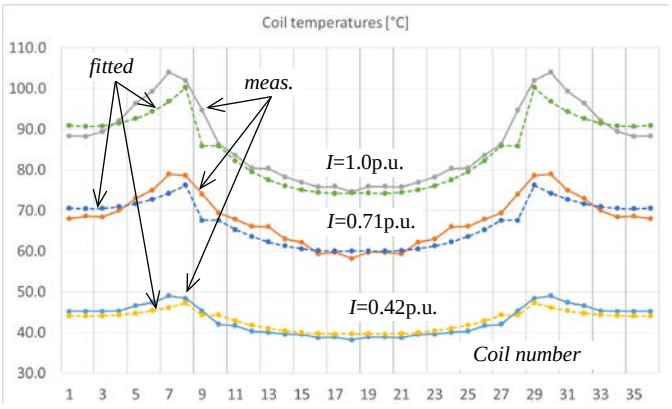

Fig. 15: Comparison between the measurements (the same of Fig. 13) and the results of the proposed fitting functions (9) for three working conditions.

IX. Conclusion

A thermal model has been developed to study the temperature distribution over the stator coils of naturally-cooled AFMs with concentrated coils. The model has been limited to the stator, i.e. the permanent magnet heating and the rotation have been neglected. Heat conduction has been studied through a 3-D analytical model. Natural convection in parallel-plate air channels has been studied to model the heat transfer from the coil surfaces. Additionally, a set of correlations has been introduced to evaluate the average Nusselt number in the stator channels between adjacent teeth, as a function of the inclined position of the channel along the machine periphery. It has been taken into account that the working condition of the coils in the lower part of the machine affects the temperature distribution in the upper part.

The study shows the following main innovative aspects:

– development of an analytical approach for the definition of a thermal model of a naturally cooled axial flux machine;
– reduced order of the thermal model, based on the iterative analysis of each wound tooth instead of the whole machine;
– fair trade-off between accuracy and calculation time of the temperature distribution, suited both for design and monitoring purposes.

The developed thermal model has been then validated by comparing the estimated temperatures and the test measurements, carried out on a 50 kW machine. The model is accurate with an average error of about 5%.

Moreover, the same thermal model allows to obtain a global convection coefficient for each wound tooth, which takes into account the global thermal exchange of the wound tooth. It is a simplified approach, which can be very useful in early design stage.

X. References

[1] H. Vansompel, A. Yarantseva, P. Sergeant and G. Crevecoeur, "An Inverse Thermal Modeling Approach for Thermal Parameter and Loss Identification in an Axial Flux Permanent Magnet Machine," in *IEEE Trans. on Ind. El.*, vol. 66, no. 3, pp. 1727-1735, March 2019.

[2] R. Boutarfa, S. Harmand, "Local convective heat transfer for laminar and turbulent flow in a rotor-stator system," *Exp. Fluids*, vol. 38, no. 2, Feb. 2005, pp. 209–221.

[3] H. Vansompel, A. Rasekh, A. Hemeida, J. Vierendeels and P. Sergeant, "Coupled Electromagnetic and Thermal Analysis of an Axial Flux PM Machine," *IEEE Trans. on Magn.*, vol. 51, no. 11, pp. 1-4, Nov. 2015.

[4] D. A. Howey, P. R. N. Childs and A. S. Holmes, "Air-Gap Convection in Rotating Electrical Machines," *IEEE Trans. on Ind. El.*, vol. 59, no. 3, pp. 1367-1375, March 2012.

[5] R. Alireza, P. Sergeant, J. Vierendeels, "Fully predictive heat transfer coefficient modeling of an AFPM synchronous machine with geometrical parameters of the magnets," *Applied Thermal Eng.* 110, 2017, pp. 1343-1357.

[6] R. Alireza, P. Sergeant, J. Vierendeels, "Development of correlations for windage power losses modeling in an axial flux permanent magnet synchronous machine with geometrical features of the magnets." *Energies* 9.12 (2016): 1009

[7] F. Marignetti, V. Delli Colli and Y. Coia, "Design of Axial Flux PM Synchronous Machines Through 3-D Coupled Electromagnetic Thermal and Fluid-Dynamical Finite-Element Analysis," *IEEE Trans. on Ind. El.*, vol. 55, no. 10, pp. 3591-3601, Oct. 2008.

[8] R. Camilleri, D. A. Howey and M. D. McCulloch, "Predicting the Temperature and Flow Distribution in a Direct Oil-Cooled Electrical Machine With Segmented Stator," *IEEE Trans. on Ind. El.*, vol. 63, no. 1, pp. 82-91, Jan. 2016.

[9] N. Rostami, M. R. Feyzi, J. Pyrhönen, A. Parviainen, M. Niemelä, "Lumped-parameter thermal model for AFPM machines." *IEEE Trans. on Mag*. Vol. 49 No. 3, pp. 1178-1184, March 2013.

[10] D. A. Howey, A. S. Holmes, K. R. Pullen, "Measurement and CFD prediction of heat transfer in air-cooled disc-type electrical machines," *IEEE Trans. Ind. Appl*., vol. 47, no. 4, pp. 1716–1723, Jul./Aug. 2011.

[11] G. Airoldi, "Numerical Investigations of Air Flow and Heat Transfer in AFPM Electrical Machines, Durham theses, Durham University, 2010. Available at Durham E-Theses Online: http://etheses.dur.ac.uk/264/

[12] Lim, Chin, Hong, "Thermal Modelling of the Ventilation and Cooling inside AFPM Generators", Durham theses, Durham University, 2010. Available at Durham E-Theses Online: http://etheses.dur.ac.uk/387/

[13] K. Latoufis, A. Rontogiannis, V. Karatasos, P. Markopoulos, N. Hatziargyriou, "Thermal and Structural Design of Axial Flux PM Generators for Locally Manufactured Small Wind Turbines," *XIII Int. Conf. on Electr. Mach. (ICEM)*, Alexandroupoli, 2018, pp. 1001-1007.

[14] M. Polikarpova, P. Ponomarev, P. Lindh, I. Petrov, W. Jara, V. Naumanen ,J. A. Tapia, J. Pyrhönen, "Hybrid Cooling Method of Axial-Flux Permanent-Magnet Machines for Vehicle Applications," *IEEE Trans. on Ind. El.*, vol. 62, no. 12, pp. 7382-7390, Dec. 2015

[15] P. Lindh, I. Petrov, A. Jaatinen-Värri, A. Grönman, M. Martinez-Iturralde, M. Satrústegui, J. Pyrhönen, "Direct Liquid Cooling Method Verified with an Axial-Flux PM Traction Machine Prototype," *IEEE Trans. on Ind. El.*, vol. 64, no. 8, pp. 6086-6095, Aug. 2017.

[16] S. T. Scowby, R. T. Dobson, M. J. Kamper, "Thermal modeling of an AFPM machine," *Applied Thermal Eng*. 24.2-3, pp. 193-207, 2004

[17] A. Di Gerlando, G. Foglia, M. Iacchetti, R. Perini, "Axial flux PM machines with concentrated armature windings: Design analysis and test validation of wind energy generators." *IEEE Trans. on Ind. El.* vol.58, no.9, 2011.

[18] R. Wrobel, P. H. Mellor, "A general cuboidal element for 3-D thermal modeling," *IEEE Trans. on Mag.* 46.8, pp. 3197-3200, 2010.

[19] N. Simpson, R. Wrobel, P.H. Mellor, "A general arc-segment element for 3-D thermal modeling." *IEEE Tr. on Mag.* 50.2, pp. 265-268, 2014.

[20] T.L. Bergman, A.S. Lavine, F.P. Incropera, D.P. Dewitt, *"Fundamentals of heat and mass transfer"* John Wiley & Sons, 2011.

[21] J. Cadafalch, A. Oliva, G. Van der Graaf, X. Albets, "Natural convection in a large, inclined channel with asymmetric heating and surface radiation," *Journal of heat transfer* 125.5, pp. 812-820, 2003.

[22] S. A. M. Said, M. A. Habib, H. M. Badr, S. Anwar, "Numerical investigation of natural convection inside an inclined parallel-walled channel," *Int. Journal for numerical methods in fluids*, 49.5, pp. 569-582, 2005.

[23] A. G. Straatman, D. Naylor, J. M. Floryan, J. D. Tarasuk, "A study of natural convection between inclined isothermal plates," *Journal of Heat Transfer*, 116.1, pp. 243-245, 1994.

[24] A. Hajji, W. M. Worek "Analysis of combined fully-developed natural convection heat and mass transfer between two inclined parallel plates," *Int. Journal of heat and mass transfer* 31.9, pp. 1933-1940, 1988

[25] A. Dalila, S. Bougoul, "Modeling of natural convection and radiative heat transfer in inclined thermosyphon system installed in the roof of a building." *Heat Transfer—Asian Research* 46.8, pp. 1148-1157, 2017.

[26] O. Manca, S. Nardini, V. Naso, "Experimental analysis of natural convection in a tilted channel." *XI Australasian Fluid Mechanics Conf.*, Vol. 1. 1992.

[27] "Heat transfer by free convection and radiation – simply shaped bodies in air and other fluids", HIS ESDU, ISBN: 9780856792045, 2003.

Pedram Shahriari Nasab received his Bachelor and Master's degree in Electrical engineering in 2012 and 2014, respectively He is currently pursuing his Ph.D. at Isfahan University of Technology, Isfahan, Iran. His main research interest includes multi-physics design of electro-mechanical systems, Electric Powertrain, and Drive and control of Electric machines

Roberto Perini (M'10) received his MS degree and the PhD in electrical engineering from the Politecnico di Milano, Milano, Italy. Currently, he is an Associate Professor at the Department of Energy at Politecnico di Milano. His interests are in the design and modeling of electrical machines and power electronics

Antonino Di Gerlando (SM' 18) received his MS degree in electrical engineering from the Politecnico di Milano, Italy, in 1981. Currently, he is a Full Professor at the Department of Energy at Politecnico di Milano. Fields of interest: design and modeling of electrical machines, converters and drive systems. He is a senior member of IEEE and a member of the Italian Association of the Electric and Electronic Engineers (AEI).

Giovanni Maria Foglia received his MS degree and the PhD in electrical engineering at Politecnico di Milano, Milano, Italy, in 1997 and 2000. Currently, he is an Assistant Professor at the Department of Energy at Politecnico di Milano, and his main field of interest is the analysis and design of PM electrical machines.

Mehdi Moallem (SM'95) received the Ph.D. degree in electrical engineering from Purdue University, West Lafayette, IN, in 1989. He has been with the Department of Electrical and Computer Engineering, Isfahan University of Technology, Isfahan, Iran since 1991. His research interests include design and optimization of electromagnetic devices, application of advance numerical techniques and intelligent systems to analysis and design of electrical machines, and power quality.